

Short communication

# Ferroelectric domain structure of lead-free potassium-sodium niobate ceramics

Rigoberto López-Juárez<sup>a,\*</sup>, Omar Novelo-Peralta<sup>a</sup>, Federico González-García<sup>b</sup>,  
Fernando Rubio-Marcos<sup>c,d</sup>, María-Elena Villafuerte-Castrejón<sup>a</sup>

<sup>a</sup> Instituto de Investigaciones en Materiales, Universidad Nacional Autónoma de México, Circuito Exterior S/N, A.P. 70-360, México, D.F., Mexico

<sup>b</sup> Departamento de Ingeniería de Procesos e Hidráulica, Universidad Autónoma Metropolitana-Iztapalapa, A.P. 55-534, 09340 México, D.F., Mexico

<sup>c</sup> Laboratoire de Science des Procédés Céramiques et de Traitements de Surface, UMR 6638 CNRS, Université de Limoges, Centre Européen de la Céramique, 12 rue Atlantis, 87068 Limoges Cedex, France

<sup>d</sup> Electroceramic Department, Instituto de Cerámica y Vidrio, CSIC, Kelsen 5, 28049 Madrid, Spain

Received 26 August 2010; received in revised form 11 February 2011; accepted 22 February 2011

Available online 3 April 2011

## Abstract

The complex domain structure of orthorhombic  $(K_{0.5}Na_{0.5})NbO_3$  (KNN) piezoelectric ceramics has been studied by SEM. The study was performed in samples prepared by microwave-hydrothermal synthesis. The identification of the domain structure has been afforded in KNN ceramics. Abnormal grain growth was observed in the microstructure of KNN ceramics, with an average grain size of 63  $\mu\text{m}$ . Most of the ferroelectric domains were 90° type with square-net and herringbone structures alternating  $a$ - $a$  and  $a$ - $c$  configurations. In addition, 180° domains were also identified arranged in the common watermark pattern.

© 2011 Elsevier Ltd. All rights reserved.

**Keywords:** Grain growth; Electron microscopy; Ferroelectric properties; Niobates

## 1. Introduction

Lead zirconate-titanate ceramics (PZT) are the most widely used piezoelectric materials until now, because of their high piezoelectric response, large scale production capability and the tailoring of their properties through composition. Recently, the European Union has published a health normative (ROH)<sup>1</sup> avoiding the use of lead (toxicity and environmental risks). Nevertheless, PZT ceramics are temporarily tolerated because of the lack of an adequate alternative. The search for alternative lead-free piezoelectric materials is now being focused on systems in which a morphotropic phase boundary (MPB) occurs. One promising alternative is based on potassium sodium niobate solid solution (KNN), due to their good electromechanical properties ( $k_p \sim 0.36$ ,  $d_{33} \sim 80$  pC/N) and Curie temperature ( $T_C \sim 420$  °C).<sup>2</sup> The crystalline symmetry and point group

of KNN at room temperature are orthorhombic and  $mm2$ , respectively, which allow to establish all possible domain wall orientations.

On the other hand, piezoelectricity appears on ferroelectric ceramics when the random ferroelectric domains are aligned through the poling process.<sup>3</sup> So, the study of ferroelectric domains in piezoelectric materials is necessary for a better understanding of their properties. In order to investigate the structure and distribution of ferroelectric domains, a number of techniques have been applied, among them, scanning probe microscopy,<sup>4</sup> environmental scanning microscopy,<sup>5</sup> optical microscopy,<sup>6</sup> transmission electron microscopy,<sup>7</sup> scanning force microscopy<sup>8</sup> and lately, scanning electron microscopy in the backscattered mode.<sup>9,10</sup>

There are several methods for revealing domains<sup>10</sup> depending upon the particular composition. For example, it is possible to study ferroelectric domains in backscattered mode by scanning electron microscopy with an appropriate sample preparation.<sup>9</sup> The ferroelectric domain pattern is generated by the interaction between the electron beam and electric dipoles inside the domains. However, it is crucial to avoid surface charge accumu-

\* Corresponding author. Tel.: +52 55 56 22 46 41x24646;

fax: +52 55 56 16 13 71.

E-mail address: [rigobertolj@yahoo.com.mx](mailto:rigobertolj@yahoo.com.mx) (R. López-Juárez).

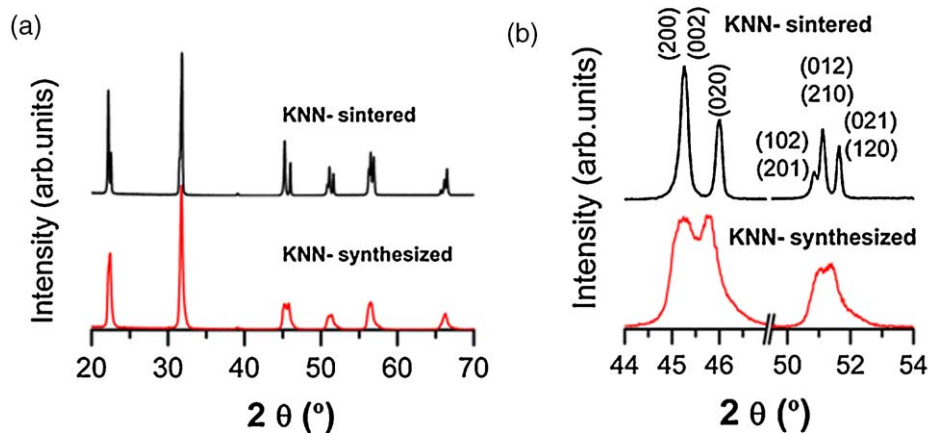


Fig. 1. (a) XRD patterns of the synthesized powders and sintered sample at 1080 °C for 4 h. (b) Magnified XRD diffraction patterns in the  $2\theta$  range 44° to 47° and 49.5° to 54° of the synthesized powders and sintered sample.

lation into the sample. This implies to find the most favorable conditions of current, voltage, etc.<sup>5,9</sup> An alternative is to reveal the ferroelectric domains by chemical etching with inorganic acids.<sup>10</sup> This is possible due to the different etching rates on positive and negative domains, giving a well defined topography, with the main drawback that it is a destructive method.

Only few papers about ferroelectric domains in KNN and related compositions, like single crystals<sup>6,11,12</sup> and polycrystalline ceramics,<sup>4,9,13</sup> are reported in the literature, all of them were performed with piezo-force microscopy. The effect of the existence of different ferroelectric domains in KNN ceramics has still not been considered in depth. This paper will present and discuss the ferroelectric domain structure in KNN polycrystalline ceramics by scanning electron microscopy on chemically etched ceramics.

## 2. Experimental procedure

The KNN powders were prepared by microwave-hydrothermal synthesis. The raw materials used were potassium hydroxide (KOH, 99.0%), sodium hydroxide (NaOH, 99.5%) and niobium oxide (Nb<sub>2</sub>O<sub>5</sub>, 99.99%). A 10 M alkaline solution was prepared in deionized water, keeping the molar ratio KOH:NaOH in 7.5:2.5. Then, 2 g of niobium oxide were added. The suspension was stirred for 2 h before pouring into a Teflon lined autoclave. The reactor was placed inside a microwave oven (MARS model, CEM Corporation) and the temperature was set at 210 °C. The heating program was as follows: a heating rate of 14 °C/min from room temperature to 210 °C, followed by a dwell of 30 min and then a cooling rate of 10 °C/min. The precipitate was washed three times with deionized water and dried at 120 °C for 2 h. With the aim of preparing a sintered sample, the dried powders were uniaxially pressed under 300 MPa in a disk-shaped sample. This sample was sintered at 1080 °C for 4 h in air. The synthesized powders and sintered pellets were analyzed by X-ray diffraction (XRD, Bruker advanced D-8 diffractometer) to confirm the crystal structure. Then, the sintered sample was chemically etched in HF (48 vol.%) at room temperature for 5 min with

no additional treatment. The sample was analyzed without any metal coating in a scanning electron microscopy (Leica STEREOSCAN 440), the current and voltage conditions were set at 0.5 nA and 20 kV, respectively. The work distance was established at 13 mm. The average grain size was determined from the SEM pictures using an image processing and analysis software (ImageJ). The surface of each grain was measured and its size was calculated in terms of equivalent-diameter for circular geometry; the average grain size (two-dimensional grain diameter) and size distribution were determined from the measurement of 400–600 grains per sample. Furthermore, an energy dispersive spectroscopy (EDS) analysis was performed in order to determine the composition of the material.

## 3. Results and discussion

The XRD patterns show the crystalline structure of the synthesized powders and sintered sample, corresponding to pure perovskite phase with orthorhombic symmetry and no secondary phases as shown in Fig. 1(a). In order to accurately identify the room temperature crystal structure of the samples, the {200} and {210} reflections were measured by slow scanning at 0.25°/min (Fig. 1(b)). The XRD peaks in the synthesized powders are quite broad, which is mainly due to the small crystal size, or another explanation is that, the perovskite structure is not completely formed. For the sintered sample, the Bragg reflections are clearly defined because of the crystal growth, shown in Fig. 1(b). Twelve polarization orientations are plausible in an orthorhombic perovskite structure due to the spontaneous polarization along  $\langle 110 \rangle_c$  direction; then, the ferroelectric domains could adopt 60°, 90°, 120° and 180° structures, as in the case of KNbO<sub>3</sub>.<sup>14</sup>

The SEM micrograph of Fig. 2(a) shows a typical KNN morphology. It can be observed that the sintered sample is composed by grains with platelet morphology that correspond to nearly cuboidal particles. It is possible to observe that the crystals have grown considerably. The pictures also revealed a bimodal grain size distribution and an average grain size of 63 μm, as shown in the inset of Fig. 2(a). The bimodality of the system may be

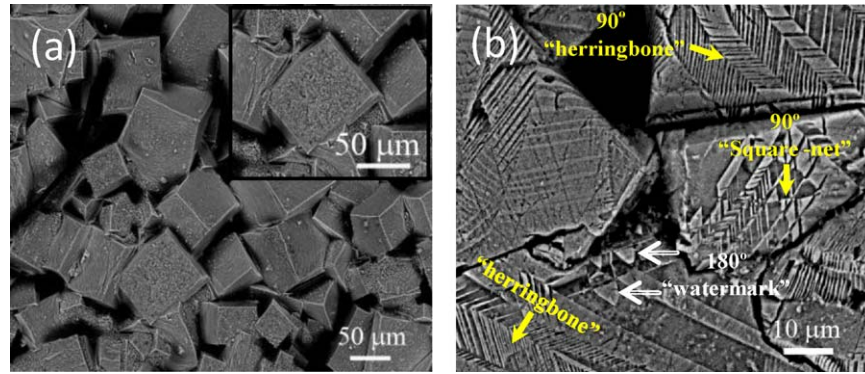


Fig. 2. Scanning electron micrographs of the sintered sample at 1080 °C for 4 h, (a) before and (b) after of the chemical etch.

attributed to the exaggerated grain growth process, as it was reported by others authors.<sup>15</sup>

In order to analyze the domain structure, several SEM images were taken over the chemically etched sample. Fig. 2(b) shows the complex structure of domains in KNN piezoelectric ceramics for the sintered and chemically etched sample. From this image the domain structure was elucidated, 90° and 180° ferroelectric domains were developed. These domains were previously observed in KNbO<sub>3</sub> and BaTiO<sub>3</sub>.<sup>14,16,17</sup>

Well-defined 90° ferroelectric domains are arranged with square-net and herringbone structures similar to BaTiO<sub>3</sub><sup>16,17</sup>, the representative microstructures of them are shown in Figs. 2(b), 3(a) and 3(b). Both, the lamellar and dagger-shaped<sup>17</sup> domains are 90° type, as indicated in Fig. 3(a). Two variants are allowed *a–a* or *a–c* depending on the viewing direction, and could be discriminated by differential etching rate along crystallographic orientations, this behaviour has been observed previously by Cheng et al.<sup>17</sup> in BaTiO<sub>3</sub>. The 90° domain structures are *a–c* type, composed of the dark and bright stripes (indicated by unfilled arrows in the framed region shown on the inset Fig. 3(b)) and suggest that they were etched heterogeneously. On the other hand, the zigzag arrangement (inset in Fig. 3(a)) of clear stripes are *a–a* type because they are etched at the same rate, as can be observed in Fig. 3(b). Furthermore, despite the fact that the sample developed a bimodal grain size distribution, it was observed that ferroelectric domains structure does not depend on the grain size.

The domain size *d*, which is defined as the mean distance between nearest domain walls, is in the range of 0.5–1 μm width and 3–7 μm long. When the thickness of 90° domains are not equal (90° *a–c* type) the mean polarization vector of the macroscopic system is an average of the polarization vector, weighted by the thickness of each domain.<sup>18</sup> Therefore, the ferroelectric properties are governed by the complex structure of domains in KNN piezoceramics, which can be controlled by domain engineering.

Fig. 3(c) shows the 180° domains. In this case, they adopt the watermark pattern<sup>17</sup> and are larger than the 90° domains (3–10 μm W × 20–40 μm L). The main feature of 180° domains is that the domain walls grow in a wavy form to reduce electrostatic energy when the head to tail coupling is violated.<sup>16–18</sup> The origin of both, 90° and 180° domains is to minimize elastic and electrostatic energy,<sup>14,16,17</sup> respectively. Another feature observed is that most domains are of the 90° type. Then, we suggest that this means that the grains are somehow under mechanical stress due to the spontaneous strain. Just as the polycrystalline ceramics grow under clamped conditions, then these stresses are evidenced in the formation of 90° domains. Another possible contribution is the presence of vacancies because of the volatilization of alkali compounds at the high sintering temperature. Addressing this issue, although an accurate chemical analysis was not performed, the EDS results revealed a homogeneous composition across the sample, and within the experimental error associated to EDS technique, the material is

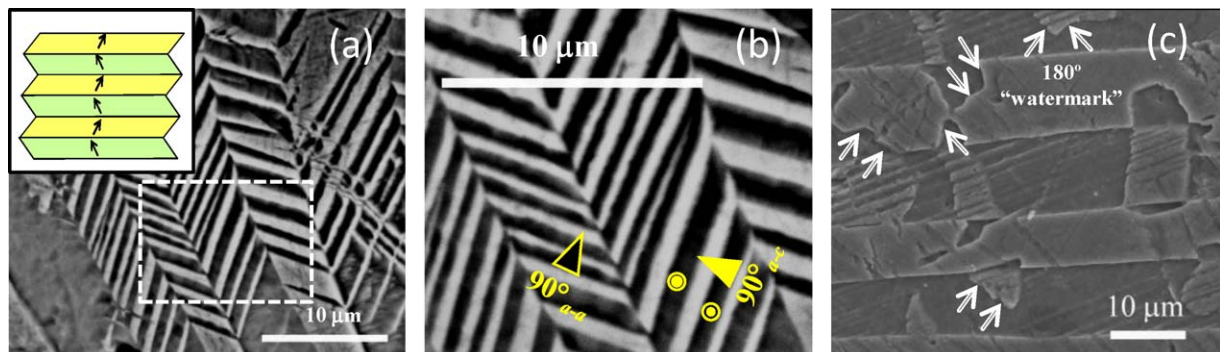


Fig. 3. Representative microstructure showing (a) lamellar 90° *a–a* and (b) dagger-shaped 90° *a–c* domains. The inset shows a scheme of the 90° wall twin structure. (c) Representative microstructure containing 180° domains.

almost in the stoichiometric composition with a slight deviation due to the Na/K losses and the corresponding oxygen vacancies.

#### 4. Conclusions

Ferroelectric domains were observed in KNN ceramics with exaggerated grain growth synthesized by microwave-hydrothermal method and sintered at 1080 °C. Two types of domains were developed, 90° and 180°. 90° domains predominated over the 180° ones. The 90° domains exhibited *a*–*a* and *a*–*c* configurations with herringbone arrangement as in BaTiO<sub>3</sub>, while the 180° domains presented watermark pattern. Domain dimensions for 90° were 0.5–1 μm width × 3–7 μm in length, while the 180° ones were 3–10 μm width and 20–40 μm in length. It is probable that the appearance of the 90° ferroelectric domains seems to be related to diminish the elastic energy developed under the growing conditions.

#### Acknowledgments

We want to thank to PAPIIT-UNAM, for supporting this research under project number IN116610-3, also to CONACyT-México for providing a PhD scholarship to R. López-Juárez. Special thanks to professor Hong-Yang Lu (National Sun Yat-Sen University) for his valuable comments and to Adriana Tejada (IIM-UNAM) for the X-ray analysis. Dr. F. Rubio-Marcos express his thanks to the MICINN (Spain) project MAT 2010-21088-C03-01 for its financial support. Finally, we wish to acknowledge the facilities provided for “Instrumentos y Equipos Falcon S.A. de C.V.” and “EQCILAB S.A. de C.V.” in the use of the Multimodal Microwave equipment CEM-MARS.

#### References

1. [http://ec.europa.eu/environment/waste/weee/index\\_en.htm](http://ec.europa.eu/environment/waste/weee/index_en.htm) (last access: 21.01.11).
2. Egerton L, Dillon DM. Piezoelectric and dielectric properties of the ceramics in the system potassium-sodium niobate. *J Am Ceram Soc* 1959;**42**:438–42.
3. Li JY, Rogan RC, Ustundag E, Bhattacharya K. Domain switching in polycrystalline ferroelectric ceramics. *Nature* 2005;**4**:776–81.
4. Herber RP, Schneider GA, Wagner S, Hoffmann M. Characterization of ferroelectric domains in morphotropic potassium sodium niobate with scanning probe microscopy. *J Appl Phys Lett* 2007;**90**:252905.
5. Zhu S, Cao W. Direct observation of ferroelectric domains in LiTaO<sub>3</sub> using environmental scanning electron microscopy. *Phys Rev Lett* 1997;**79**:2558–62.
6. Bencan A, Tchernychova E, Godec M, Fisher J, Kosec M. Compositional and structural study of a (K<sub>0.5</sub>Na<sub>0.5</sub>)NbO<sub>3</sub> single crystal prepared by solid state crystal growth. *Microsc Microanal* 2009;**15**:435–40.
7. Kling J, Tan X, Jo W, Kleebe HJ, Fuess H, Rodel J. In situ transmission electron microscopy of electric field-triggered reversible domain formation in bi-based lead-free piezoceramics. *J Am Ceram Soc* 2010;1–4, doi:10.1111/j.1551-2916.2010.03778.x.
8. Jungk T, Soergel E. Contrast mechanism for visualization of ferroelectric domains with scanning force microscopy. *Ferroelectrics* 2006;**334**:29–34.
9. Gruner D, Shen Z. Direct scanning electron microscopy imaging of ferroelectric domains after ion milling. *J Am Ceram Soc* 2010;**93**:48–50.
10. Soergel E. Visualization of ferroelectric domains in bulk single crystals. *Appl Phys B* 2005;**81**:729–52.
11. Inagaki Y, Kakimoto K, Kagomiya I. Crystal growth and ferroelectric property of Na<sub>0.5</sub>K<sub>0.5</sub>NbO<sub>3</sub> and Mn-doped Na<sub>0.5</sub>K<sub>0.5</sub>NbO<sub>3</sub> crystals grown by floating zone method. *J Eur Ceram Soc* 2010;**30**:301–6.
12. Lin D, Li Z, Zhang S, Xu Z, Yao X. Dielectric/piezoelectric properties and temperature dependence of domain structure evolution in lead free Na<sub>0.5</sub>K<sub>0.5</sub>NbO<sub>3</sub> single crystal. *Solid State Commun* 2009;**149**:1646–9.
13. Cho JH, Lee YH, Kim BI. Domain structure of orthorhombic (Li,K,Na)NbO<sub>3</sub> ceramics. *J Ceram Process Res* 2010;**11**:237–40.
14. Hirohashi J, Yamada K, Kamio H, Uchida M, Shichijyo S. Control of specific domain structure in KNbO<sub>3</sub> single crystals by differential vector poling method. *J Appl Phys* 2005;**98**:034107.
15. Zhen Y, Li JF. Abnormal grain growth and new core-shell structure in (K,Na)NbO<sub>3</sub>-based lead-free piezoelectric ceramics. *J Am Ceram Soc* 2007;**90**:3496–502.
16. Arlt G, Sasko P. Domain configuration and equilibrium size of domains in BaTiO<sub>3</sub> ceramics. *J Appl Phys* 1980;**51**:4956–60.
17. Cheng SY, Ho NJ, Lu HY. Transformation-induced twinning: the 90° and 180° ferroelectric domains in tetragonal barium titanate. *J Am Ceram Soc* 2006;**89**:2177–87.
18. Pérez R, García JE, Albareda A, Gomis V, Ochoa DA. Motion of 90° and 180° ferroelectric domain wall structures. *Mech Mater* 2010;**42**:374–82.